Int. J. Advance Soft Compu. Appl, Vol. 18, No. 2, July 2026
Print ISSN: 2710-1274, Online ISSN: 2074-8523

Variable-order fractional calculus, chaotic systems, numerical methods, fractional derivatives, nonlinear dynamics

Ghadah Alhawael[1]

[1]Department of Basic Sciences, Common First Year Deanship, King Saud University, P.O.Box 145111, Riyadh 11362, Saudi Arabia.
e-mail: Galhawil@ksu.edu.sa

Abstract

Recently, the V-O-F fractional differential operators have become quite popular for modelling nonlinear dynamical systems with hereditary effects and memory features. However, the V-O-F operator is more suitable for nonlinear dynamical systems with chaotic properties, even though the integer-order derivative operator is a great method for comprehending the behavior of some ordinary differential equations. Here, we present a generalized numerical method to simulate the solution of a broad class of V-O-F differential equations, based on the theorem of fractional calculus and Lagrange interpolation polynomials. The technique may effectively take into account various kernels, including the Atangana-Baleanu-Caputo kernel, the Caputo kernel, and the Caputo-Fabrizio kernel. We use our suggested numerical method to simulate the dynamics of nonlinear chaotic models, specifically a circuit model and a time-varying financial system model.

Keywords: *variable-order fractional calculus, chaotic systems, numerical methods, fractional derivatives, nonlinear dynamics.*

1 Introduction

Recently, Fractional calculus has garnered a lot of interest as an extension of the traditional calculus, which allows the differentiation and integration processes to be generalized for non-integer order real numbers. This new generalized mathematical tool has been shown to be a useful and flexible tool for modeling nonlinear systems, which can be more accurately modeled compared to traditional integer order systems [1,2,3].

Fractional order modeling can be used as an efficient tool for modeling systems in which memory effects, heredity, and temporal interactions over large time scales are dominant. Such effects are often found in a wide variety of systems, including engineering processes, biological systems, and physical systems, as presented in [4,5,6,7]. In contrast with integer order modeling, fractional order modeling can capture the effects of the past states of the systems, which makes it more efficient for modeling the systems' behaviors over time. In fact, it has been shown that fractional order modeling can successfully simulate the systems' behaviors, including nonlinear and chaotic oscillations, with high accuracy compared with integer order modeling, as presented in [8,9,10,11]. This efficiency makes

Received 4 February 2026; Accepted 20 May 2026

it more useful for the needs of the present technology and industry, in which memory effects cannot be neglected.

Fixed-order fractional models may become inadequate when the memory characteristics of a system change over time, since a constant derivative order cannot fully represent evolving memory effects or dynamically varying system behavior. To overcome this limitation, variable-order fractional derivatives have been developed, in which the order of differentiation is allowed to vary with time, spatial position, or other system-related parameters. Such flexibility makes it possible for the variable-order approach to effectively model processes that have properties like non-stationarity, adaptation, and heterogeneity. Thus, the use of variable-order fractional calculus can provide a more practical and effective way to model complicated real-world phenomena [12,13,14,15,16].

In the last few decades, significant interest in the study of variable-order fractional chaotic systems has been observed owing to their improved ability to model not only the memory effect but also complex chaotic dynamics. As opposed to their fixed-order counterparts, which cannot consider evolving dynamics of the system, the variable-order models consider the changes in the nature of the system and therefore become a perfect way to model nonlinear processes that possess time varying properties. Hence, such an approach becomes more efficient and allows describing physical and engineering problems related to nonstationary processes. Despite that, it should be noted that the analytical examination of variable-order fractional chaotic systems is complicated due to their high level of nonlinearity and time varying order of derivatives. Therefore, to explore dynamics of such systems, stability issues, and chaos phenomena, numerical methods have proven themselves to be extremely helpful. Besides, the rising popularity of variable-order fractional models may be explained by the fact that such an approach shows good results when applied in practice [17,18,19].

The V-O-F Models have been widely used in various scientific and engineering disciplines. The V-O-F models have been effectively utilized in the non-linear epidemiology models, where the diffusion of some behaviors, such as smoking and pediculosis, takes place with time-dependent memory effect. These models have also found significant use in control theory and engineering for the analysis and development of control strategies for the stability of systems that are dynamically changing. The development of advanced solution techniques for these models further highlights the significance and applicability of V-O-F models [20,21,22,23]. Recent studies have highlighted the growing importance of fractional calculus and advanced numerical methods in accurately modeling complex dynamical systems [24,25,26,27].

Variable-order fractional financial systems are used to describe financial systems realistically by considering time-varying memory effects and time-varying financial market dynamics, which cannot be realistically captured by conventional integer-order or fixed-order fractional financial models. Financial systems are highly complex in nature, and financial models are characterized by many complexities, including long memory, volatility clustering, regime switching, and nonlinear interactions among financial variables. By considering time-varying order in fractional financial models, variable-order fractional financial models can realistically capture time-varying financial market dynamics, changes in financial structure, changes in investor behavior, and changes in financial uncertainty levels, thereby enabling a realistic analysis of financial systems, including financial forecasting, stability analysis, chaotic financial systems [28,29,30,31].

The variable-order fractional financial system, as proposed initially in [32].is a mathematical description of the dynamic relationships between the four essential economic variables: production, money supply, bonds, and labor force. The combination of these variables is a summary of the essential economic laws that govern the evolutionary dynamics of financial markets. The variable-order fractional financial system is defined by the operator $D_{0,t}^{\alpha(t)}$ as follows:

$$\begin{cases} D_{0,t}^{\alpha(t)} x_1(t) = x_3(t) + (x_2(t) - a)x_1(t), \\ D_{0,t}^{\alpha(t)} x_2(t) = 1 - bx_2(t) - x_1^2(t), \\ D_{0,t}^{\alpha(t)} x_3(t) = -x_1(t) - cx_3(t), \end{cases} \tag{1}$$

In this financial system, the dynamic of the interest rate $x_1(t)$ is controlled by two main variables: the imbalance between investments and savings, as well as the structural changes caused by fluctuations in the prices of goods. The investment demand $x_2(t)$ is assumed to be proportional to the investment rate, illustrating the responsiveness of investments to economic conditions. The price exponent $x_3(t)$ is a description of the dynamics of prices within the commercial market and is controlled by the imbalance between supply and demand [33].

To improve the descriptive capabilities of the classical financial system, the integer-order derivatives are replaced by a variable-order derivative. This modification allows the financial system to incorporate the effects of memory-dependent dynamics, thus enabling the financial system to effectively deal with economic dependencies over time.

Figure 1 depicts three different fractional operators of variable order in the financial model, namely Caputo, Caputo-Fabrizio (CF), and Atangana-Baleanu in Caputo sense (ABC). The conventional Caputo fractional operator is associated with a power law kernel along with classical initial conditions, which makes it suitable for representing the phenomenon of long memory and heredity in financial modeling. However, the CF fractional operator involves a non-singular kernel with an exponential kernel function that represents short memory and rapidly varying phenomena without any singularity. Together, these operators offer complementary perspectives for modeling variable-order fractional financial systems.

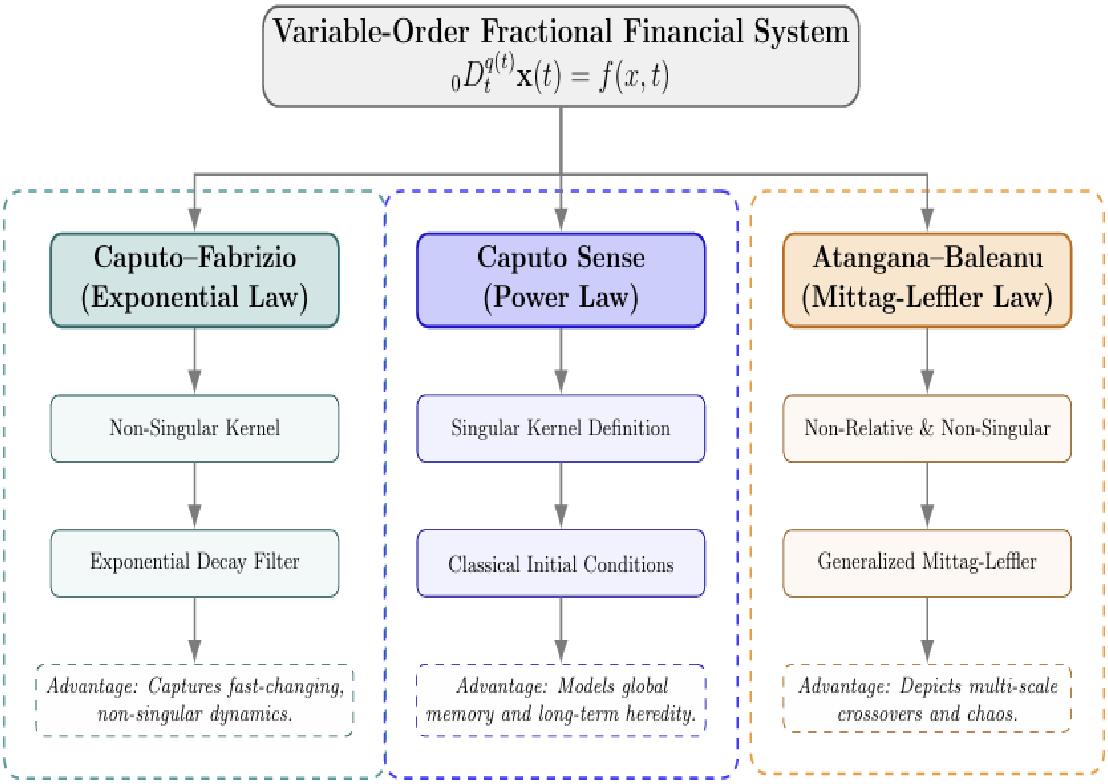

Figure 1: Classification and modeling advantages of the three variable-order fractional operators.

The main contributions to the present work can be briefly described as follows:

- A generalized numerical framework has been developed to handle variable-order fractional differential equations with various kernel forms, such as power-law, exponential-law, and Mittag-Leffler kernels.
- New numerical approaches, based on the fundamental theorem of fractional calculus and the Lagrange polynomial interpolation method, have been developed for the variable-order fractional derivatives of the Caputo, CF, and ABC operators.
- The developed numerical approaches have been applied to simulate the solutions of nonlinear chaotic systems, such as the chaotic financial system and the memcapacitor-based circuit chaotic oscillator.
- A comparative analysis of the numerical solutions obtained with the variable-order fractional operators has been carried out to assess the performance and convergence properties of the numerical solutions.
- The impact of the V-O-Fs on the dynamics of the chaotic system has been studied, particularly during the transition between chaotic and regular dynamics.
- Numerical results validate the performance and accuracy of the developed numerical approaches, which can be effectively used to investigate the complex variable-order fractional chaotic systems.

2 Mathematical Analysis of the Fractional-Order financial system

In this section, we analyze system 1. The objective is to investigate the dynamical behavior of the proposed system.

2.1 Equilibrium Points Analysis

To find the equilibrium points of the system, we set the fractional derivatives to zero:

$$D_{0,t}^{\alpha(t)}\, x_1(t) = D_{0,t}^{\alpha(t)}\, x_2(t) = D_{0,t}^{\alpha(t)}\, x_3(t) = 0$$

From the third equation, we find:

$$x_3 = -x_1$$

Substituting $x_3 = -x_1$ into the first equation gives:

$$-x_1 + (x_2 - 1)x_1 = 0$$
$$x_1(x_2 - 2) = 0$$

This leads to two distinct cases:

Case A: $x_1 = 0$

If $x_1 = 0$, then $x_3 = 0$.

Substituting $x_1 = 0$ into the second equation:

$$1 - 0.1\,x_2 - 0^2 = 0 \rightarrow 0.1\,x_2 = 1 \rightarrow x_2 = 10$$

This yields the first equilibrium point:

$$E_0 = (0, 10, 0)$$

Case B: $x_1 = 0$

If $x_1 \geq 0$, then the expression inside the parentheses must be zero, so:

$$x_2 - 2 = 0 \rightarrow x_2 = 2$$

Substituting $x_2 = 2$ into the second equation:

$$1 - 0.1(2) - x_1^2 = 0$$
$$1 - 0.2 - x_1^2 = 0 \rightarrow x_1^2 = 0.8$$
$$x_1 = \pm\sqrt{0.8} = \pm\frac{2\sqrt{5}}{5}$$

Since $x_3 = -x_1$, we get $x_3 = \sqrt{0.8}$. This yields two additional equilibrium points:

$$E_1 = \left(\sqrt{0.8}, 2, -\sqrt{0.8}\right) \quad \text{and} \quad E_2 = \left(-\sqrt{0.8}, 2, \sqrt{0.8}\right)$$

2.2 Jacobian Matrix at $\boldsymbol{E_0}$

The general Jacobian matrix of the system is:

$$J(x_1, x_2, x_3) = \begin{bmatrix} x_2 - 1 & x_1 & 1 \\ -2x_1 & -0.1 & 0 \\ -1 & 0 & -1 \end{bmatrix}$$

Evaluating this matrix at the equilibrium point $E_0 = (0, 10, 0)$:

$$J(E_0) = \begin{bmatrix} 10 - 1 & 0 & 1 \\ 0 & -0.1 & 0 \\ -1 & 0 & -1 \end{bmatrix} = \begin{bmatrix} 9 & 0 & 1 \\ 0 & -0.1 & 0 \\ -1 & 0 & -1 \end{bmatrix}$$

2.3 Characteristic Equation at $\boldsymbol{E_0}$

To find the eigenvalues associated with E_0, we solve det $(\lambda I - J(E_0)) = 0$:

$$\begin{bmatrix} \lambda - 9 & 0 & -1 \\ 0 & \lambda + 0.1 & 0 \\ 1 & 0 & \lambda + 1 \end{bmatrix} = 0$$

Expanding along the second row:

$$(\lambda + 0.1)[(\lambda - 9)(\lambda + 1) - (-1)(1)] = 0$$

$$(\lambda + 0.1)[\lambda^2 - 8\lambda - 9 + 1] = 0$$

$$(\lambda + 0.1)(\lambda^2 - 8\lambda - 8) = 0$$

One eigenvalue is immediately apparent:

$$\lambda_1 = -0.1$$

The other two eigenvalues are roots of the quadratic equation $\lambda^2 - 8\lambda - 8 = 0$ Using the quadratic formula:

$$\lambda = \frac{8 \pm \sqrt{(-8)^2 - 4(1)(-8)}}{2} = \frac{8 \pm \sqrt{64 + 32}}{2} = \frac{8 \pm \sqrt{96}}{2} = 4 \pm 2\sqrt{6}$$

The three eigenvalues at $\boldsymbol{E_0}$ are:

$$\lambda_1 = -0.1$$

$$\lambda_2 = 4 + 2\sqrt{6} \approx 8.899$$

$$\lambda_3 = 4 - 2\sqrt{6} \approx -0.899$$

2.4 Stability Analysis of E_0

According to fractional-order stability theory, the equilibrium point is progressively stable if all eigenvalues satisfy the condition:

$$|\arg(\lambda_i)| > \frac{\alpha\pi}{2} \text{ for } i = 1,2,3$$

Analyzing the arguments of the derived eigenvalues:

- $\lambda_1 = -0.1$ is a negative real number, so $|\arg(\lambda_1)| = \pi > \frac{\alpha\pi}{2}$
- $\lambda_3 = 4 - 2\sqrt{6} \approx -0.899$ is a negative real number, so $|\arg(\lambda_3)| = \pi > \frac{\alpha\pi}{2}$
- $\lambda_2 = 4 + 2\sqrt{6} \approx 8.899$ positive real number, so its argument is exactly zero:

$$|\arg(\lambda_2)| = 0 > \frac{\alpha\pi}{2}$$

Therefore, the equilibrium point $E_0 = (0, 10, 0)$ is unstable (specifically, exhibiting saddle behavior) for any fractional order $0 < \alpha < 1$.

The classical definitions of stability are not applicable to the variable-order fractional systems. The theorem of stability for constant order, e.g., Matignon's theorem, is not applicable when the derivative order $\alpha(t)$ is time-varying. The rigorous theoretical justification should be obtained using the fractional Lyapunov direct method. A positive-definite Lyapunov function for the system is defined. The system is asymptotically stable if the variable-order derivative of this function satisfies it, where 'c' is a positive constant. The memory kernel is time-varying.

3 Definition and Analysis of the Variable-Order Fractional Operators

This section defines the variable-order fractional derivatives with time-varying order $\alpha(t)$ used to capture dynamic memory effects. It is also necessary to consider the present theoretical debates concerning the properties of non-singular fractional operators like those used in the Caputo-Fabrizio or Atangana-Baleanu formulation. According to the literature [34], the above operators possess some particular limitations, especially that their value for $t = 0$ is exactly zero; hence, these models impose some unnecessary limitations upon certain problems and cannot be used in solving initial value problems that require satisfying the traditional statement of the fundamental theorem of fractional calculus. Nevertheless, when considered within the framework of this investigation, the operators mentioned here are used only within a variable-order setting with a continuously varying order $\alpha(t)$. These non-singular fractional operators are not regarded here as derivatives in a classical sense but only as memory operators having time dependence [35].

3.1 Liouville-Caputo Variable-Order Derivative

The Liouville–Caputo fractional derivative with variable order (t) uses a singular power-law kernel and is well suited for modeling systems with heavy-tailed memory. It is defined as [36]: ${}_{0}^{C}D_{t}^{\alpha(t)}g(t) = \frac{1}{\Gamma(1-\alpha(t))}\int_0^t (t-\rho)^{-\alpha(t)}\dot{g}(\rho)d\rho,\ 0 < \alpha(t) \le 1$ (2)

3.2 Caputo-Fabrizio Variable-Order Derivative (CF)

The Caputo–Fabrizio derivative in the Liouville–Caputo sense (CF) uses a non-singular exponential kernel to model smoothly decaying memory effects. For $0 < \alpha(t) < 1$, it is defined as [36]:

$$ {}_{0}^{CF}D_{t}^{\alpha(t)}g(t) = \frac{(2-\alpha(t))M(\alpha(t))}{2(1-\alpha(t))}\int_0^t \exp\left[-\alpha(t)\frac{(t-\rho)}{1-\alpha(t)}\right]\dot{g}(\rho)d\rho \quad (3) $$

where the normalization function is given by: $M(\alpha(t)) = \frac{2}{2-\alpha(t)}$

3.4 Atangana-Baleanu Variable-Order Derivative (ABC)

The Atangana–Baleanu fractional derivative (ABC) uses a non-local, non-singular Mittag–Leffler kernel to model complex nonlinear dynamics [37]:

$$ {}_{0}^{ABC}D_{t}^{\alpha(t)}g(t) = \frac{B(\alpha(t))}{1-\alpha(t)}\int_0^t E_{\alpha(t)}\left[-\alpha(t)\frac{(t-\rho)^{\alpha(t)}}{1-\alpha(t)}\right]\dot{g}(\rho)d\rho, 0 < \alpha(t) \le 1 \quad (4) $$

where the normalization function $B(\alpha(t))$ is defined as: $B(\alpha(t)) = 1 - \alpha(t) + \frac{\alpha(t)}{\Gamma(\alpha(t))}$

and $E_{\alpha(t)}(.)$ denotes the one-parameter Mittag-Leffler function, which is defined by the following infinite series:

$$ E_{\alpha(t)}(z) = \sum_{k=0}^{\infty} \frac{z^k}{\Gamma(\alpha(t)k+1)} \quad (5) $$

4. Model Development in the Fractional Variable Framework

The variable-order fractional differential operators are used to create an effective mathematical tool in modeling nonlinear fractional systems, including chaotic systems. In this section, the suggested system is described using three different variable-order fractional derivatives, namely the Caputo, CF, and ABC fractional derivatives. These variable-order fractional derivatives are connected with different kernels, including the power-law, exponential-law, and Mittag-Leffler kernels, respectively.

$$\begin{cases} D_{0,t}^{\alpha(t)} x_1(t) = x_3(t) + (x_2(t) - a)x_1(t), \\ D_{0,t}^{\alpha(t)} x_2(t) = 1 - bx_2(t) - x_1^2(t), \\ D_{0,t}^{\alpha(t)} x_3(t) = -x_1(t) - cx_3(t), \end{cases} \tag{6}$$

where $D_{0,t}^{\alpha(t)} x_1(t)$ denotes the variable-order fractional (V-O-F) derivative of order $\alpha(t) \in (0,1]$ with respect to time t. such that:

- C represents the Caputo sense,
- CF represents the Caputo-Fabrizio sense,
- ABC represents the Atangana-Baleanu-Caputo sense.

where $\alpha(t) \in (0,1]$ is the V-O-F taken in the Atangana-Baleanu-Caputo sense and t is time.

5 Numerical Schemes for Variable-Order Fractional Financial System

This section derives the approximate scheme [38 ,40] for the proposed systems 6 are obtained using three different fractional operators: the Caputo, Caputo-Fabrizio (CF), and Atangana-Baleanu-Caputo (ABC) derivatives.
Consider system (1), where $D_{0,t}^{\alpha(t)}$ represents the fractional derivative in the sense of Caputo, CF, or ABC. The system is subject to the initial condition

$$x(0) = x_0 = (x_{1,0}, x_{2,0}, x_{3,0})^T$$

Let $x = (x_1, x_2, x_3) \in$. The system can be written in the compact form

$$D_{0,t}^{\alpha(t)} x(t) = F(t, x(t)), t \in [0, T]$$

where $F\big(t, x(t)\big) = (f_1, f_2, f_3)^T$ denotes the nonlinear vector field.

5.1 Discretization and Numerical Schemes

To approximate the solution, we consider an equi-spaced mesh over the interval $[0, a]$ with time step

$$h = \Delta t = 0.001.$$

Let

$$t_n = nh, \qquad n = 0,1,2,$$

and denote by $x_{i,n}$ the numerical approximation of $x_i(t_n)$ for $i = 1,2,3$.

5.2 Caputo Fractional Scheme

Using the Caputo fractional derivative, the numerical approximation for x_i is given by

$$x_{i,n+1} = x_i(0) + \frac{1}{\Gamma(\alpha(t))}\sum_{m=0}^{n}\left[\frac{h^{\alpha(t)} f_i(t_m, x_{1,m}, x_{2,m}, x_{3,m})}{\alpha(t)(\alpha(t)+1)}\Phi_1(t) - \frac{h^{\alpha(t)} f_i(t_{m-1}, x_{1,m-1}, x_{2,m-1}, x_{3,m-1})}{\alpha(t)(\alpha(t)+1)}\Phi_2(t)\right] \quad (7)$$

Where

$$\Phi_1(t) = (n+1-m)^{\alpha(t)}(n-m+2+\alpha(t)) - (n-m)^{\alpha(t)}(n-m+2+2\alpha(t))$$

$$\Phi_2(t) = (n+1-m)^{\alpha(t)+1} - (n-m)^{\alpha(t)}(n-m+1+\alpha(t))$$

Similar expressions can be obtained for x_2 and x_3.

5.3 Caputo-Fabrizio (CF) Scheme

For the Caputo-Fabrizio fractional derivative, the numerical approximation is expressed as

$$x_{i,n+1} = x_{i,n} + \left[\frac{(2-\alpha(t))(1-\alpha(t))}{2} + \frac{3h}{4}\alpha(t)(2-\alpha(t))\right] f_i(t_n, x_{1,n}, x_{2,n}, x_{3,n}) - \left[\frac{(2-\alpha(t))(1-\alpha(t))}{2} + \frac{h}{4}\alpha(t)(2-\alpha(t))\right] f_i(t_{n-1}, x_{1,n-1}, x_{2,n-1}, x_{3,n-1}) \quad (8)$$

for $i = 1,2,3$.

5.4 Atangana-Baleanu-Caputo (ABC) Scheme

For the ABC fractional operator, the numerical scheme is given by

$$x_{i,n+1} = x_i(0) + \frac{1-\alpha(t)}{B(\alpha(t))} f_i(t_n, x_{1,n}, x_{2,n}, x_{3,n}) + \frac{1}{B(\alpha(t))\Gamma(\alpha(t))(\alpha(t)+1)}\sum_{m=0}^{n}[\, h^{\alpha(t)} f_i(t_m, x_{1,m}, x_{2,m}, x_{3,m})\Phi_1(t) - h^{\alpha(t)} f_i(t_{m-1}, x_{1,m-1}, x_{2,m-1}, x_{3,m-1})\Phi_2(t)] \quad (9)$$

5.5 Remarks on the Variable-Order Effects

To study the impact of the V-O-F on the system dynamics, three different forms of $\alpha(t)$ are considered, each representing a distinct type of temporal variation:

Case 1 $\alpha(t) = 0.95 + 0.05\, cos\left(\frac{t}{5}\right)$ represents a periodic variation of the fractional order, allowing the investigation of oscillatory memory effects in the system.

Case 2 $\alpha(t) = \frac{1}{1+\exp(-t)}$ describes a monotonic logistic-type variation, modeling situations where the memory effect gradually increases and approaches a stable level over time.

Case 3 $\alpha(t) = tanh(t+1)$ provides a smooth nonlinear transition toward a bounded value, reflecting processes where the fractional order changes rapidly at first and then stabilizes.
For obtaining profound insights on the impact of these variable-order functions on hereditary characteristics of the systems, as well as the topology of the chaotic regime, one must analyze their contribution under the perspective of dynamic modulation and temporal nonlocality of phase space. So, in Case 1 (periodic variation), the continuously changing values of the fractional order led to the dynamical "breathing" of the phase space of the attractor when the system dynamically moves between extreme levels of memory retention and dissipation. This results in continuous change of effective dimensions which forces the system through a set of intermittently chaotic and periodic regimes. In its turn, Case 2 (logistic monotonic variation) represents the physical process which corresponds to unidirectional evolution of the depth of memory when the variable order gradually changes its value and reaches saturation. Thus, the volume of the phase space is permanently deformed by such processes, and the trajectory of the system, starting from the unstable transient stage, ends up with a stable chaotic attractor. Lastly, in Case 3 (rapid saturating transition), an early shock is observed when there is a violent change in memory properties, followed by saturation.
These examples demonstrate periodic, monotonic, and saturating phenomena in the behavior of fractional order which provides insight into the way in which different types of variable orders affect the dynamics of the systems.
As discussed in [30], three different forms of $\alpha(t)$ are studied for examining their effect on the dynamics of the system as follows: (i) periodic behavior, Case 1, for exploring oscillatory effects in memory; (ii) monotonic logistic curve, Case 2, for investigating the effect of gradually stabilized memory; and (iii) saturating nonlinear behavior, Case 3.

6 Numerical Experiments

We perform numerical simulations of the variable-order fractional financial system with step size $h = 0.001$ and initial conditions $x_1(0) = 2, x_2(0) = -1, zx_3(0) = 1$. Where $a = 1, b = 0.1, and\ c = 1$, Three representative cases for the V-O-F $\alpha(t)$ are considered: Case (1), Case (2), and Case (3). The numerical solutions exhibit chaotic behavior in all three cases, highlighting the strong impact of variable-order dynamics on the system.

6.1 Variable-Order Fractional Financial System under the C Fractional Scheme

Tables [1] to [3] show the V-O-F-based numerical solutions to the variable-order fractional financial system under three cases. The state variables $x_1(t)$, $x_2(t)$, and $x_3(t)$, decrease over time and $x_1(t)$, tend to stabilize, $x_2(t)$, tend to a less negative value, and $x_3(t)$, change to negative values. The solutions under all cases are similar, indicating the stability and reliability of the V-O-F approach in computing solutions to this system over $t \in [0,1]$.

Table 1: Numerical outcomes of System 6 (Case 1) under Caputo Derivative

Time	$x_1(t)$	$x_2(t)$	$x_3(t)$
0.0	2.000000000000000	-1.000000000000000	1.000000000000000
0.1	1.724424745320694	-1.213372334660323	0.753526074362359
0.2	1.428146254435692	-1.348939179917771	0.532262173361732

0.3	1.164425261273389	-1.402807141572373	0.358779572817987
0.4	0.940924162702502	-1.399183078874255	0.224968140365386
0.5	0.756665937353346	-1.357094500644614	0.123230019834761
0.6	0.606958924709642	-1.290071652934141	0.046993243525755
0.7	0.486133686781775	-1.207241163152676	-0.009180823036689
0.8	0.388807614632160	-1.114592415002226	-0.049682556991202
0.9	0.310346575143726	-1.016004107936338	-0.078007813330325
1.0	0.246946103413197	-0.913974703950905	-0.096919943339741

Table 2: Numerical outcomes of System 6 (Case 2) under Caputo Derivative

Time	$x_1(t)$	$x_2(t)$	$x_3(t)$
0.0	2.000000000000000	-1.000000000000000	1.000000000000000
0.1	1.697041116953062	-1.229070242212097	0.731699886019895
0.2	1.403155796835585	-1.356395196406918	0.514987504925266
0.3	1.142920759534802	-1.404337741125111	0.345329911225470
0.4	0.923022996552212	-1.396692719309057	0.214639079825023
0.5	0.742027570959925	-1.351969781660979	0.115400352798669
0.6	0.595090440716826	-1.283260585982099	0.041142664196284
0.7	0.476539317039024	-1.199370966691310	-0.013475753974148
0.8	0.381048887790159	-1.106071406220735	-0.052761011169213
0.9	0.304058280219521	-1.007096291026715	-0.080139173437995
1.0	0.241833135435834	-0.904850472120444	-0.098317266346809

Table 3: Numerical outcomes of System 6 (Case 3) under Caputo Derivative

Time	$x_1(t)$	$x_2(t)$	$x_3(t)$
0.0	2.000000000000000	-1.000000000000000	1.000000000000000
0.1	1.700287639023131	-1.226062841172108	0.734903321848866
0.2	1.395936203531142	-1.353124507417639	0.512054396501047
0.3	1.134506947393636	-1.393835871827257	0.343162968521869
0.4	0.918760386867925	-1.378126441339662	0.215909064438180
0.5	0.744306811583702	-1.326677982949800	0.120740196649772
0.6	0.604467924143067	-1.253070246722077	0.050195635046403
0.7	0.492601843013214	-1.165965878808404	-0.001495841189844
0.8	0.402959337303294	-1.070821097383409	-0.038770484711204
0.9	0.330860232360038	-0.971060552627529	-0.065030987069602
1.0	0.272603912269224	-0.868836052980195	-0.082888777621829

6.2 Chaotic Behavior of Fractional financial System C

Figures 2–4 depict the chaotic behavior of the V-O-F financial system for Cases 1-3. For all cases, it is observed that the state variables of the system display complex and non-periodic behavior with sensitive dependence on initial conditions, which is reminiscent of chaotic behavior. For Case 1, it is observed that the state variables of the system display dense and overlapping behavior, which is typical of highly nonlinear interactions in the system. In Cases 2 and 3, it is observed that the state variables of the system are exhibiting spread-out behavior with similar patterns. These observations confirm that the financial system is exhibiting chaotic behavior for different parameter values. Moreover, these results also confirm the effectiveness of the V-O-F financial model for modeling the intricate behavior of financial systems.

This is illustrated in Figures 5 below for the three different cases under study. From Figure 5 above, it is evident that the time evolution of the Lyapunov Exponents (LE) of the system reveals its chaotic nature. All three different scenarios result in the stabilization of the spectrum with a positive LE $(LE_1 > 0)$ and zero or negative LEs, the characteristic features of chaotic dynamics. Figure 6 shows the respective bifurcation diagrams for the state x_2 as a function of b, showing chaotic dynamics at low values of b.

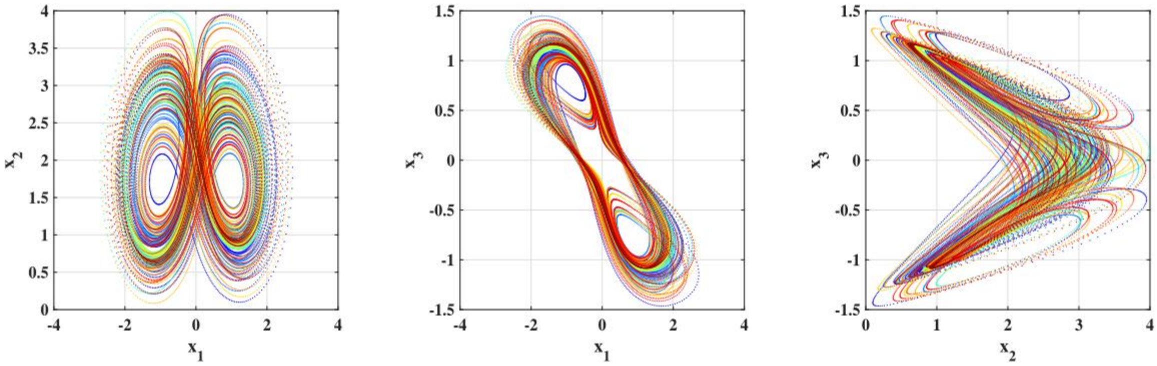

Figure 2: Phase portraits of Case 1 depicting chaotic behavior in system 6

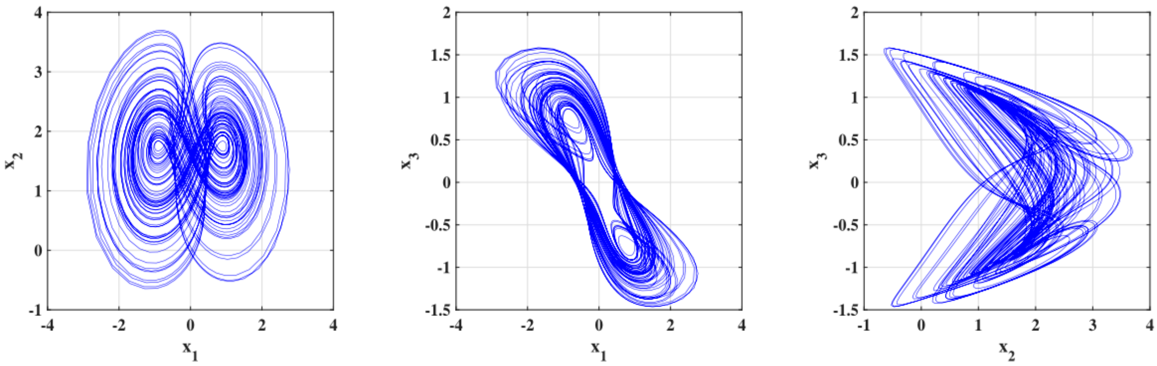

Figure 3: Phase portraits of Case 2 depicting chaotic behavior in system 6

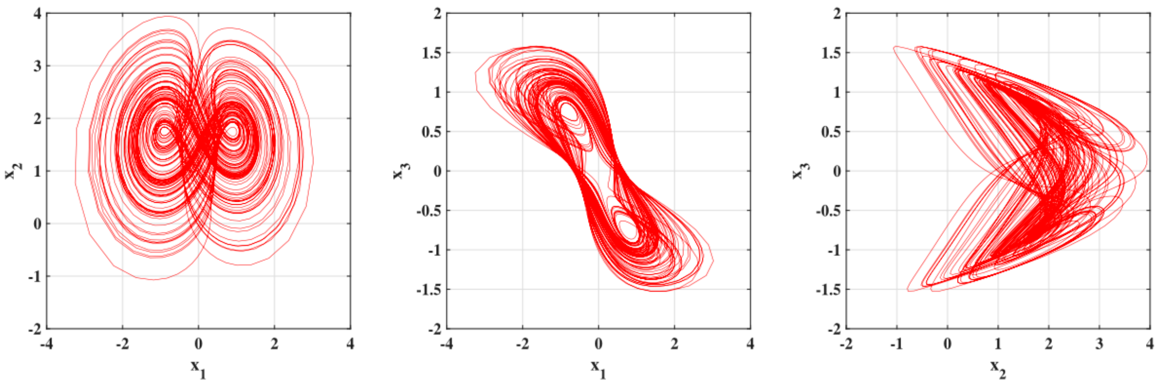

Figure 4: Time evolution of the Lyapunov Exponents (LE) for Cases (1-3)

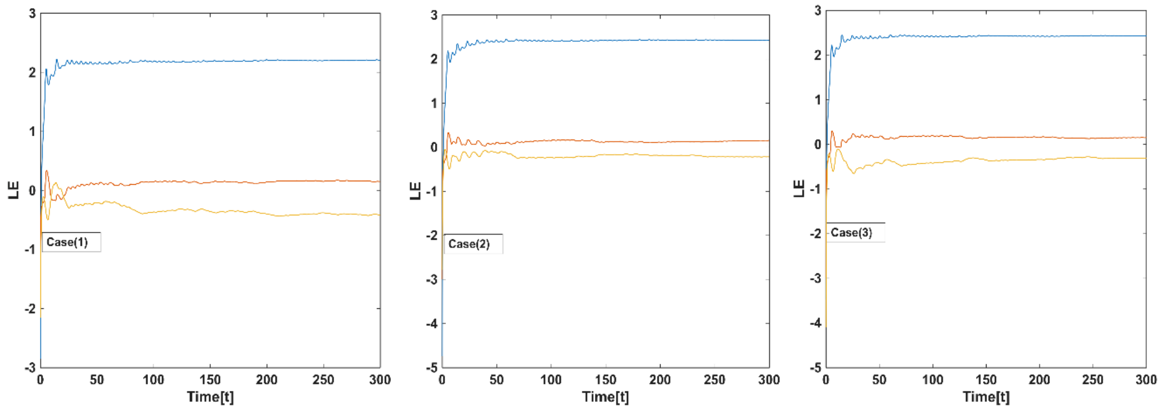

Figure 5: Time evolution of the Lyapunov Exponents (LE) for Cases (1-3)

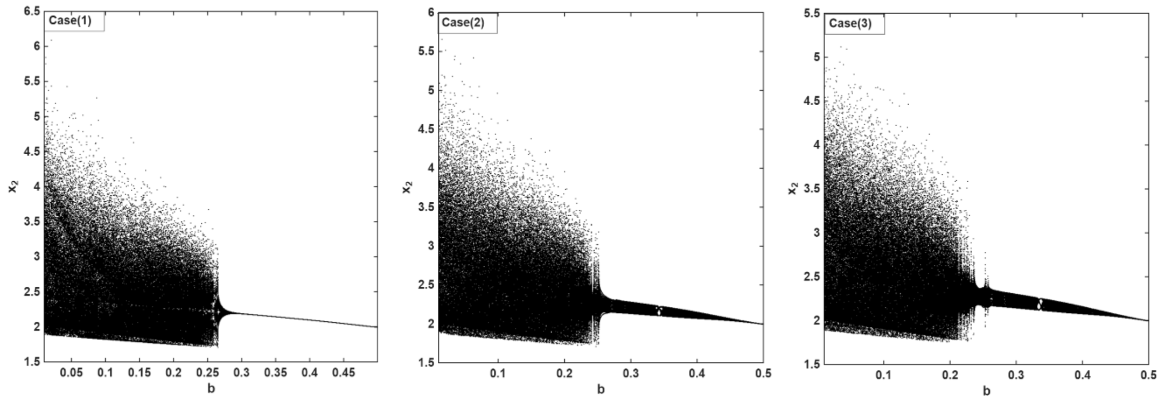

Figure 6: Bifurcation diagrams of the state variable x2 versus parameter b for Cases (1-3)

6.3 Variable-Order Fractional Financial System under the CF Fractional Scheme

The corresponding numerical data presented in Tables 4 - 6 illustrate the dynamics of the variable-order fractional financial system under the CF derivative for Cases 1-3. In all cases, $x_1(t)$ is decreasing over time, $x_2(t)$ is negative and tends to zero, and $x_3(t)$ is decreasing steadily from its initial value. The data illustrate the typical damping and memory effects of the fractional-order system, and the more significant decay in Cases 2 and 3 confirms the efficiency of the CF approach in modeling the fractional financial system.

Table 4: Numerical outcomes of System 6 (Case1) under CF Derivative

Time	$x_1(t)$	$x_2(t)$	$x_3(t)$
0.0	2.000000000000000	-1.000000000000000	1.000000000000000
0.1	1.852166204469266	-1.060777121680733	0.883875050061693
0.2	1.721260539445120	-1.110277446369389	0.782424377974070
0.3	1.593679511503398	-1.152543367264745	0.685376176494074
0.4	1.470448602696494	-1.185886475333039	0.593867756810375
0.5	1.352403151764514	-1.209555125460355	0.508624138026356
0.6	1.240217296659660	-1.223485943351809	0.430033997677553
0.7	1.134397218716747	-1.228085358712813	0.358223411703635
0.8	1.035271543652639	-1.224054090442035	0.293120860142234
0.9	0.942993023437463	-1.212253018906266	0.234511900371267
1.0	0.857553615185788	-1.193605144633153	0.182083825845616

Table 5: Numerical outcomes of System 6 (Case2) under CF Derivative

Time	$x_1(t)$	$x_2(t)$	$x_3(t)$
0.0	2.000000000000000	-1.000000000000000	1.000000000000000
0.1	1.832182416732932	-1.141686321256652	0.843754182505833
0.2	1.678715392443102	-1.239854123753716	0.717034615795036
0.3	1.529088417802785	-1.312079200348966	0.603906040668906
0.4	1.386378928771702	-1.361583250456383	0.503438897456361
0.5	1.252519870113164	-1.391661302048166	0.414627372853339
0.6	1.128540899700378	-1.405437209723990	0.336443120207710
0.7	1.014802699629024	-1.405728734903003	0.267874654108536
0.8	0.911199364986884	-1.394991317246279	0.207954126279810
0.9	0.817320184704590	-1.375312623734479	0.155773905183452
1.0	0.732571720451567	-1.348436307020923	0.110495434554900

Table 6: Numerical outcomes of System (Case3) under CF Derivative

Time	$x_1(t)$	$x_2(t)$	$x_3(t)$
0.0	2.000000000000000	-1.000000000000000	1.000000000000000
0.1	1.788782136549095	-1.086592308569718	0.834964345809017
0.2	1.661786133480226	-1.127927869686234	0.738165671222016
0.3	1.538139540927947	-1.162719620473662	0.645539051156767
0.4	1.418879613979073	-1.189377955666955	0.558179993307815
0.5	1.304818768982004	-1.207178877040582	0.476790011176915
0.6	1.196582493187162	-1.216041141133951	0.401747897783074
0.7	1.094618775045545	-1.216324361870964	0.333179602406483
0.8	0.999200628193684	-1.208664679091806	0.271020662667871
0.9	0.910435017619512	-1.193848978016961	0.215068963403123
1.0	0.828281062885273	-1.172723264540805	0.165027829534236

6.4 Chaotic Behavior of Fractional financial System CF

The phase portrait diagrams for Cases 1-3 of the variable-order fractional financial system are shown in Figures 7 - 9. It can be seen that there are typical fractional-order dynamics for the system, and the spiral convergence of the system can be found. With the increase of the case numbers, the attractors of the system are stretched and complex.

The chaotic behavior and stability of the model under different parameters are described in Figures 10 and 11. The graph shown in Figure 9 represents the dynamic time plot of the Lyapunov Exponents (LE). This result verifies the existence of chaos with rapid stabilization of the highest positive exponent value ($LE_1 > 0$). On the other hand, the bifurcation behavior of the state variable x_2 for varying b values is depicted in Figure 10. These bifurcation diagrams support the findings of LE, which exhibit a dense chaotic area for small values of b that eventually evolve to stable orbits or equilibria through inverse bifurcations.

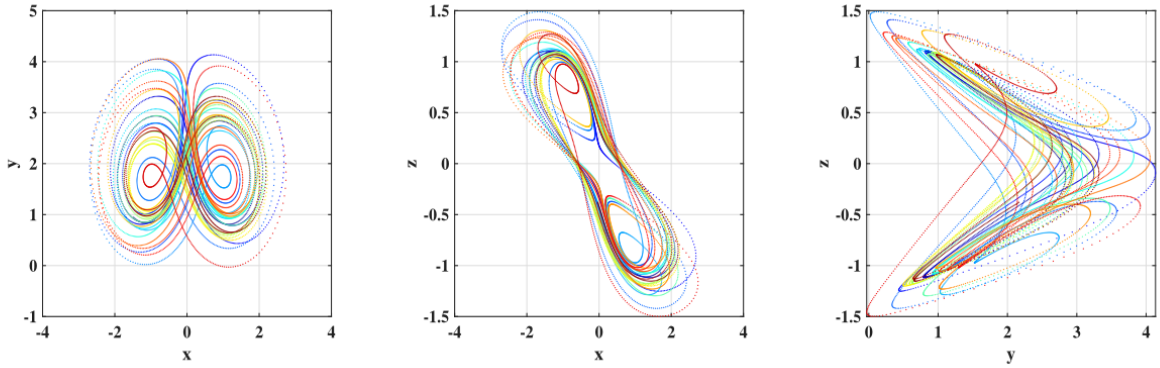

Figure 7: Phase portraits of Case1depicting chaotic behavior in system 6

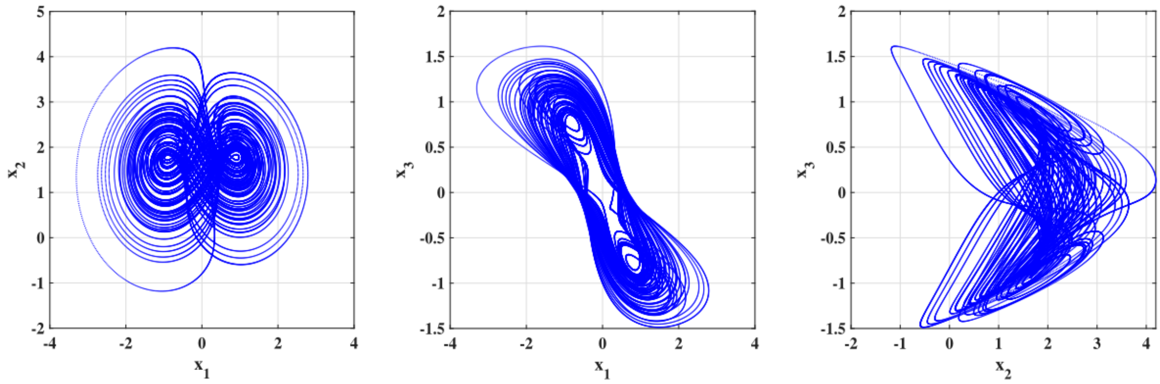

Figure 8: Phase portraits of Case2 depicting chaotic behavior in system 6

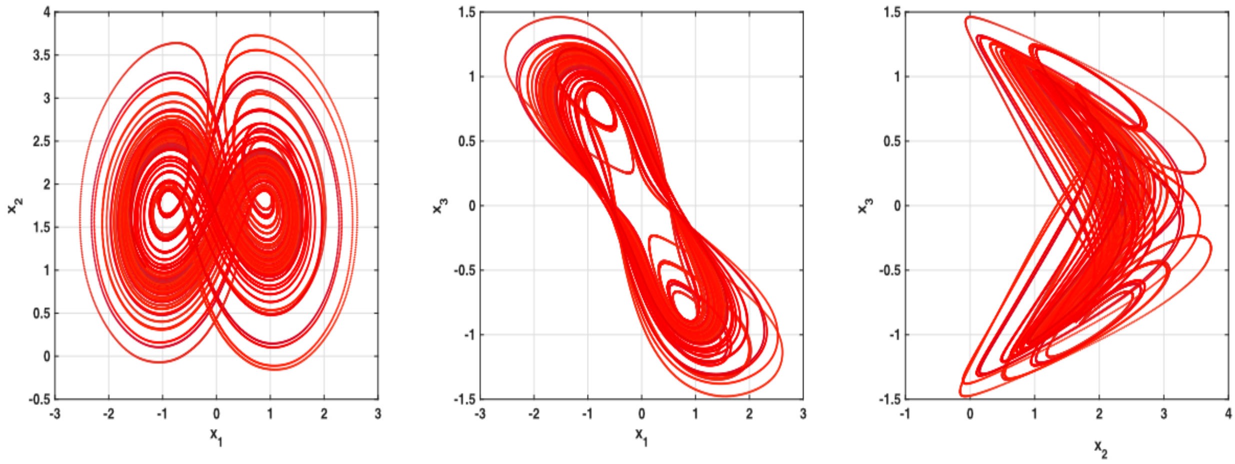

Figure 9: Phase portraits of Case3 depicting chaotic behavior in system 6

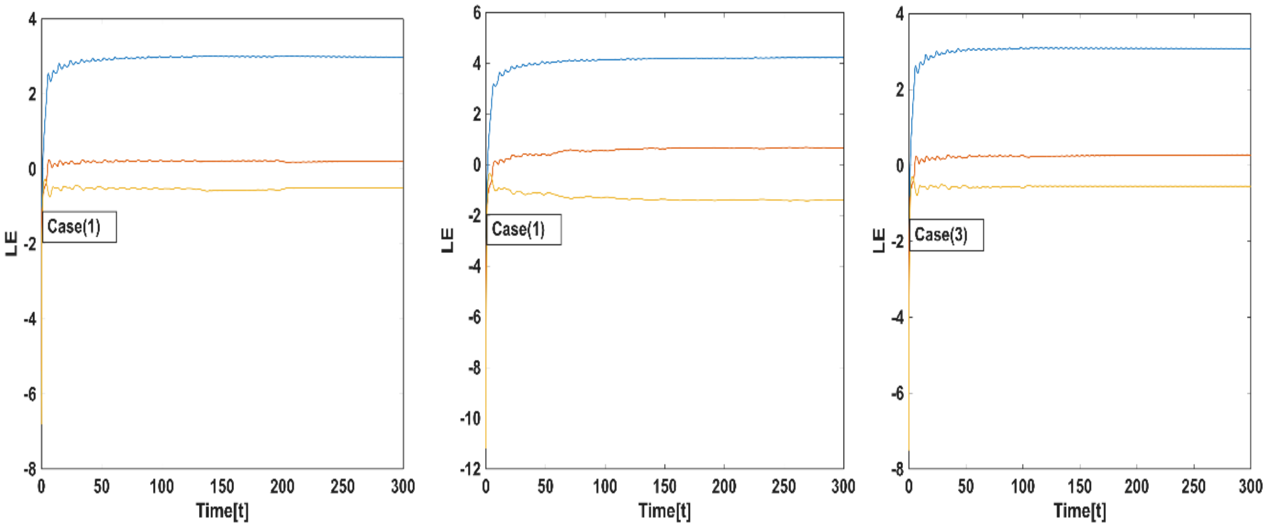

Figure 10: Time evolution of the Lyapunov Exponents, confirming chaotic dynamics via a positive maximum exponent.

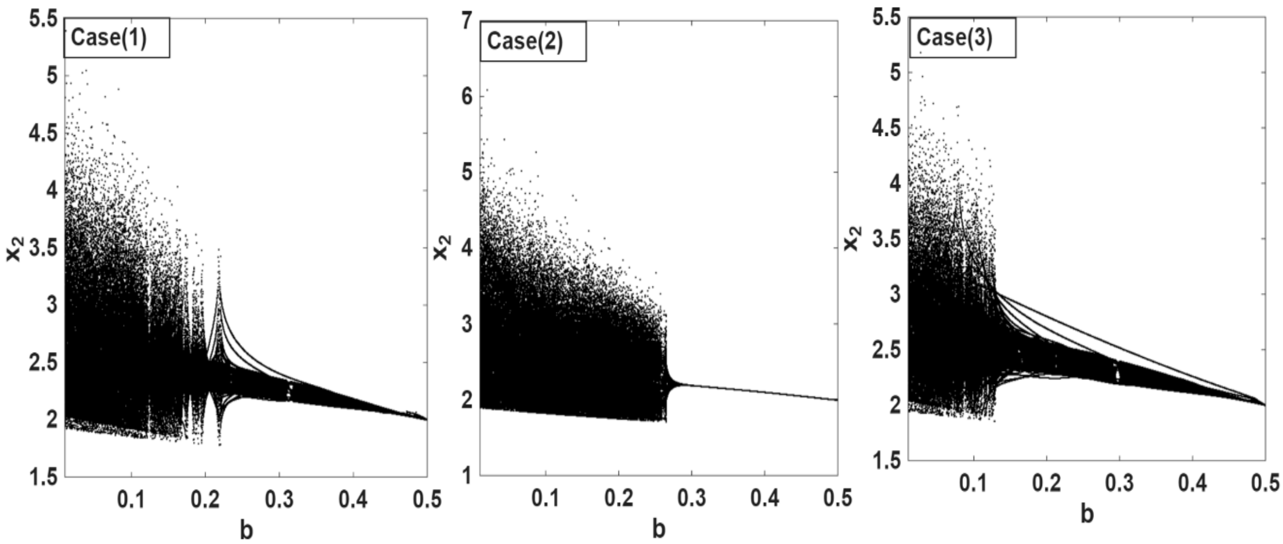

Figure 11: Bifurcation diagrams versus parameter b, mapping the transition from a chaotic region to stable states.

6.5 Variable-Order Fractional Financial System under the CF Fractional Scheme

The solutions of System 6 using the ABC derivative for Cases 1–3 have been presented in Tables 7- 9. It is found that $x_1(t)$ becomes smaller with time, whereas $x_2(t)$ increases, and $x_3(t)$ also decreases in all three cases, although some small oscillations exist for . $x_3(t)$The third case shows a slower rate of decay.

Table 7: Numerical outcomes of System 6 (Case 1) under ABC Derivative

Time	$x_1(t)$	$x_2(t)$	$x_3(t)$
0.0	2.000000000000000	-1.000000000000000	1.000000000000000
0.1	1.455762029492741	-1.340708028652927	0.551518535519785
0.2	0.960742212493873	-1.401786977328402	0.236661760847000
0.3	0.620250575160089	-1.297460667140333	0.053773751573720

0.4	0.397597764267888	-1.124039315645222	-0.046025990837698
0.5	0.252736927675522	-0.924352434276632	-0.095247845105058
0.6	0.157516684982617	-0.716310886844044	-0.114334235951864
0.7	0.094056058345407	-0.507336968136365	-0.115938785714587
0.8	0.051209480547734	-0.300502330671519	-0.107860531681110
0.9	0.021963698169226	-0.097053726486361	-0.094883055720635
1.0	0.001818228176729	0.102538089478199	-0.079905636780178

Table 8: Numerical outcomes of System 6 (Case 2) under ABC Derivative

Time	$x_1(t)$	$x_2(t)$	$x_3(t)$
0.0	2.000000000000000	-1.000000000000000	1.000000000000000
0.1	1.374561224624782	-1.317051798050836	0.509820303997550
0.2	0.947799183054705	-1.312793204749109	0.241217767940336
0.3	0.658116435138515	-1.191873619316955	0.080749573542384
0.4	0.463214880601654	-1.022082612904296	-0.012959436087917
0.5	0.330815917008662	-0.832927563310367	-0.065172049732912
0.6	0.239511825004589	-0.637407479083763	-0.091592581454884
0.7	0.175588651909296	-0.441340386842633	-0.102111811399155
0.8	0.130254064992160	-0.247346048674694	-0.103024218941169
0.9	0.097791707272003	-0.056582159401757	-0.098361522246319
1.0	0.074416597847432	0.130476381708597	-0.090709725471872

Table 9: Numerical outcomes of System 6 (Case 3) under ABC Derivative

Time	$x_1(t)$	$x_2(t)$	$x_3(t)$
0.0	2.000000000000000	-1.000000000000000	1.000000000000000
0.1	1.074807677384052	-1.073511032682446	0.310313755420307
0.2	0.911559134998432	-0.951181375896807	0.212905524212941
0.3	0.794575171476623	-0.826627797788957	0.135353612095623
0.4	0.697751119383628	-0.693652475931867	0.073000597804045
0.5	0.616177640161282	-0.551690632417853	0.022151253010529
0.6	0.547514514760706	-0.401488508809232	-0.019136179824459
0.7	0.490268201935585	-0.244397745690994	-0.052308871320868
0.8	0.443242278320522	-0.082011082870196	-0.078690227118605
0.9	0.405378054037199	0.084046357892494	-0.099567601330059
1.0	0.375733897858252	0.252232879100592	-0.116184866604117

6.6 Chaotic Behavior of Fractional financial System ABC

The phase portraits presented in Figures 12 - 13, and 14 illustrate the evolution of a chaotic system across three distinct scenarios, projected onto the $x_1 - x_2$, $x_1 - x_3$, and $x_2 - x_3$ planes. Figure 12 (Case 1) utilizes a multi-colored gradient to highlight the temporal progression and orbital divergence characteristic of strange attractors, while Figures 13 and 14 (Cases 2 and 3) employ uniform blue and red color schemes, respectively, to focus on the geometric density of the trajectories.

Both Figures 15 and 16 investigate the dynamical process and sensitivity to parameters of the system. The LE spectra in Figure 15, on the other hand, show that the system indeed possesses chaotic attractors for all cases, characterized by an asymptotic (+, 0, -) signature where the largest value of the LE is positive ($LE_1 > 0$). In particular, the bifurcation diagrams of the state variable x_2 for the parameter interval $b \in [0,0.5]$ plotted in Figure 15 completely agree with the results obtained via LE analysis. Chaotic regions are clearly identified with dense bands at smaller values of b, until undergoing a transition beyond the critical range of $b \in [0.22, 0.26]$.

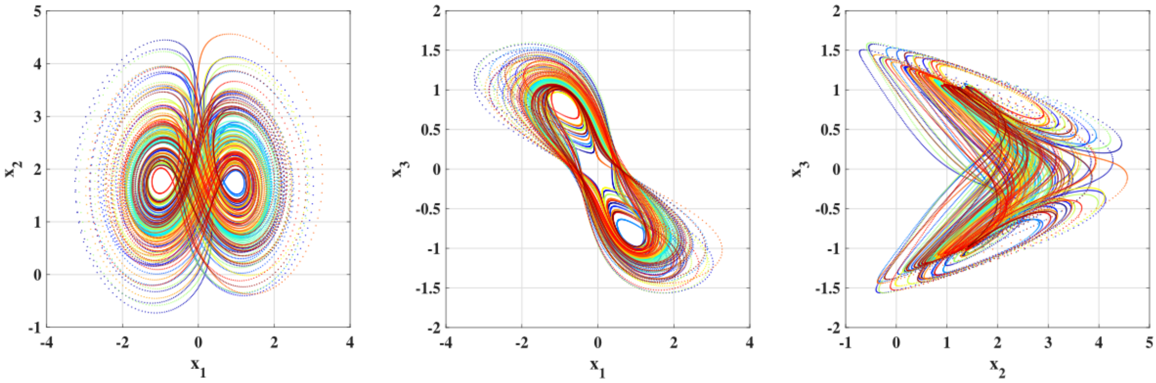

Figure 12: Phase portraits of Case 1 depicting chaotic behavior in system 6

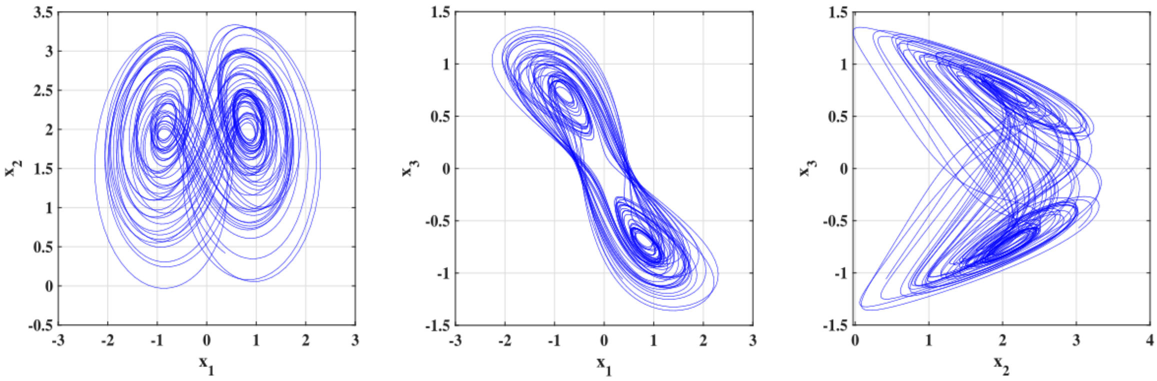

Figure 13: Phase portraits of Case 2 depicting chaotic behavior in system 6

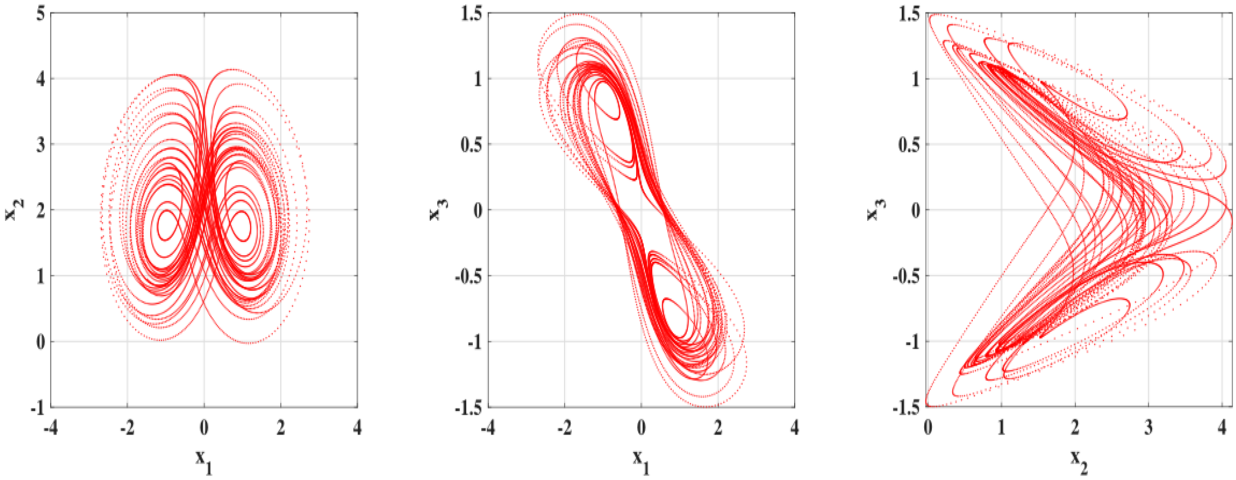

Figure 14: Phase portraits of Case 3 depicting chaotic behavior in system 6

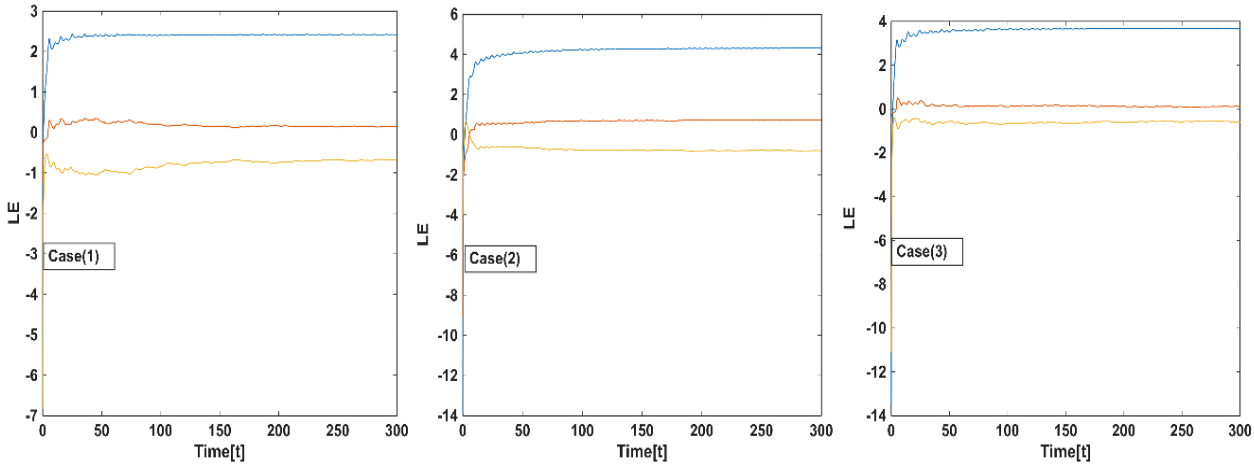

Figure 15: Lyapunov exponent evolution showing chaos via a positive maximum.

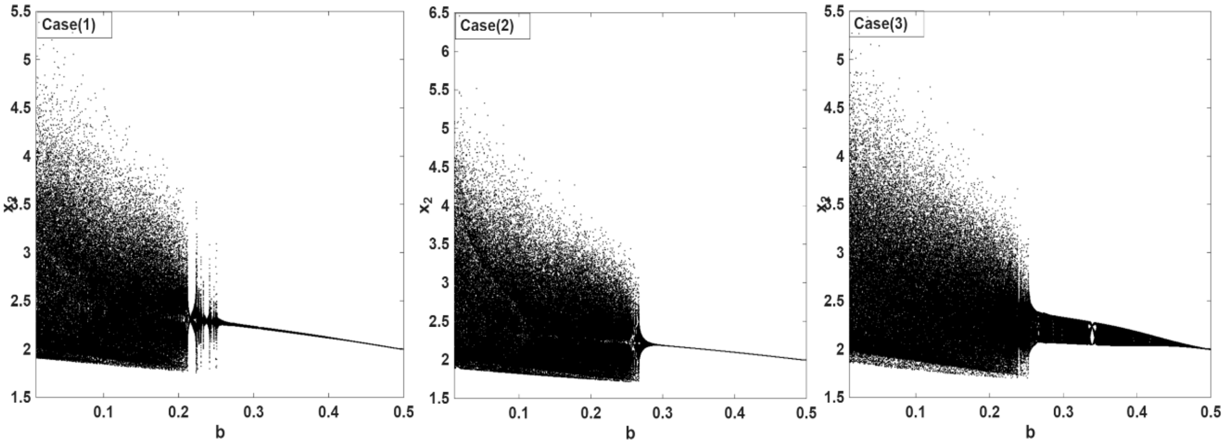

Figure 16: Time evolution of the Lyapunov exponents for three cases, showing convergence and a positive maximum exponent indicative of chaotic behavior.

Table 10: Determination of the numerical accuracy of the Caputo schema for Case 1.

t	$\Delta = \lvert C_{0.01} - C_{0.001}\rvert$			$\Delta = \lvert C_{0.001} - C_{0.0001}\rvert$		
	Δx1	**Δx2**	**Δx3**	**Δx1**	**Δx2**	**Δx3**
0.5	1.46384×10^{-2}	5.12472×10^{-3}	7.82967×10^{-3}	1.46408×10^{-3}	5.26688×10^{-4}	7.70941×10^{-4}
0.6	1.18685×10^{-2}	6.81107×10^{-3}	5.85058×10^{-3}	1.18392×10^{-3}	6.96523×10^{-4}	5.72366×10^{-4}
0.7	9.59437×10^{-3}	7.87020×10^{-3}	4.29493×10^{-3}	9.54167×10^{-4}	8.02841×10^{-4}	4.16838×10^{-4}
0.8	7.75873×10^{-3}	8.52101×10^{-3}	3.07845×10^{-3}	7.69034×10^{-4}	8.67884×10^{-4}	2.95728×10^{-4}
0.9	6.28829×10^{-3}	8.90782×10^{-3}	2.13136×10^{-3}	6.21039×10^{-4}	9.06308×10^{-4}	2.01887×10^{-4}
1.0	5.11297×10^{-3}	9.12423×10^{-3}	1.39732×10^{-3}	5.03011×10^{-4}	9.27606×10^{-4}	1.29547×10^{-4}

Table 11: Determination of the numerical accuracy of the CF schema for Case 1.

t	$\Delta = \lvert CF_{0.01} - CF_{0.001} \rvert$			$\Delta = \lvert CF_{0.001} - CF_{0.0001} \rvert$		
	Δx_1	Δx_2	Δx_3	Δx_1	Δx_2	Δx_3
0.5	4.75844×10^{-2}	2.37625×10^{-3}	3.18341×10^{-2}	8.619619×10^{-3}	8.052315×10^{-4}	5.888083×10^{-3}
0.6	4.36348×10^{-2}	7.44480×10^{-3}	2.82861×10^{-2}	7.892161×10^{-3}	1.714997×10^{-3}	5.251373×10^{-3}
0.7	3.97784×10^{-2}	1.17610×10^{-2}	2.50438×10^{-2}	7.183091×10^{-3}	2.491304×10^{-3}	4.667823×10^{-3}
0.8	3.60709×10^{-2}	1.53894×10^{-2}	2.21002×10^{-2}	6.502406×10^{-3}	3.144656×10^{-3}	4.136669×10^{-3}
0.9	3.25580×10^{-2}	1.84040×10^{-2}	1.94429×10^{-2}	5.858344×10^{-3}	3.687663×10^{-3}	3.656101×10^{-3}
1.0	2.92726×10^{-2}	2.08819×10^{-2}	1.70560×10^{-2}	5.256822×10^{-3}	4.133781×10^{-3}	3.223551×10^{-3}

Table 12: Determination of the numerical accuracy of the ABC schema for Case 1.

t	$\Delta = \lvert ABC_{0.01} - ABC_{0.001} \rvert$			$\Delta = \lvert ABC_{0.001} - ABC_{0.0001} \rvert$		
	Δx_1	Δx_2	Δx_3	Δx_1	Δx_2	Δx_3
0.5	1.05230×10^{-2}	1.77924×10^{-2}	3.10530×10^{-3}	1.12466×10^{-3}	1.73277×10^{-3}	3.36767×10^{-4}
0.6	7.22369×10^{-3}	1.80221×10^{-2}	1.09466×10^{-3}	8.65906×10^{-4}	1.69439×10^{-3}	1.78102×10^{-4}
0.7	5.12036×10^{-3}	1.78519×10^{-2}	6.87043×10^{-5}	7.49809×10^{-4}	1.60426×10^{-3}	1.03816×10^{-4}
0.8	3.78043×10^{-3}	1.75071×10^{-2}	7.05648×10^{-4}	7.32226×10^{-4}	1.48585×10^{-3}	7.64173×10^{-5}
0.9	2.94040×10^{-3}	1.70856×10^{-2}	1.02063×10^{-3}	7.87469×10^{-4}	1.34986×10^{-3}	7.08490×10^{-5}
1.0	2.43967×10^{-3}	1.66307×10^{-2}	1.14545×10^{-3}	9.01485×10^{-4}	1.20168×10^{-3}	6.98938×10^{-5}

6 Conclusion

The current study achieves its goal of developing and implementing numerical methods for solving V-O-F differential equations. Relying on the fundamental theorem of fractional calculus and Lagrange interpolation, the developed scheme provides an accurate solution for the numerical evaluation of fractional operators governed by different kernel definitions such as singular power-law (Caputo), nonsingular exponential-law (CF), and nonlocal Mittag-Leffler-law (ABC). We utilized the algorithms described above to explore the dynamics of highly nonlinear complex systems like the chaotic financial system and memcapacitive oscillators. The simulations reveal the stability and high precision of the proposed scheme, especially when using fine time step sizes. A comparison study among the Caputo, CF, and ABC operators reveals unique advantages and disadvantages for each one regarding modeling chaotic dynamics. More importantly, our numerical results demonstrate the effect of changing the fractional derivative order in time on the dynamics of the whole system, causing bifurcation and switching between chaotic and stable behavior. Future work will explore new fractional models [41,42] and compare them with other numerical methods [43,44].

References

[1] Younas, U., Hussain, E., Muhammad, J., Sharaf, M., & Meligy, M. E. (2025). Chaotic structure, sensitivity analysis and dynamics of solitons to the nonlinear fractional longitudinal wave equation. International Journal of Theoretical Physics, 64(2), 42.

[2] Mumtaz, A., Masood, K., Shakeel, M., & Shah, N. A. (2025). Exploring complex dynamics in nonlinear Riemann wave models using fractional calculus-based expansion. Scientific Reports.

[3] Alsubaie, N. E., El Guma, F., Musa, A. G., Abdali, H. A., Awadalla, M., & Alosaimi, B. (2026). Comparative evaluation of Cox regression and machine learning approaches for survival prediction in stage IV lung cancer. Discover Computing, 29(1), 102.

[4] Abdulkream Alharbi, S., Abdoon, M. A., Saadeh, R., Alsemiry, R. D., Allogmany, R., Berir, M., & El Guma, F. (2024). Modeling and analysis of visceral leishmaniasis dynamics using fractional-order operators: A comparative study. Mathematical Methods in the Applied Sciences, 47(12), 9918–9937.

[5] Alhawael, G., Abdoon, M. A., Khashan, K. H., & Elgezouli, D. E. (2025). Chaos analysis of the fractional Genesio-Tesi system with constant and variable-order dynamics. Mathematics, 13(24), 3992.

[6] Kadri, I., Gündoğdu, H., Abdoon, M. A., Afif, E., Modawy, Y. M., & Cattani, C. (2025). Numerical approach to fractional model for dispersion, dissipation, and diffusion with a logistic reaction. International Journal of Advances in Soft Computing & Its Applications, 17(3).

[7] Kadri, I., Gundogdu, H., Modawy, Y. M., Imam, A., Helal, K. A., Elshamy, I., & Tahir, R. A. (2025). A comparative analysis of the non-linear time fractional Whitham-Broer-Kaup equations under Aboodh decomposition transform. European Journal of Pure and Applied Mathematics, 18(3), 6626.

[8] Elbadri, M., Ashmaig, M. A., Hassan, A. A., Hdidi, W., Barakat, H. M., Al-Mutairi, G. S., & Abdoon, M. A. (2025). Exploring stability and chaos in the fractional-order Arneodo system via Grünwald–Letnikov scheme. Mathematics, 13(24), 3925.

[9] Allogmany, R., Almuallem, N. A., Alsemiry, R. D., & Abdoon, M. A. (2025). Exploring chaos in fractional order systems: A study of constant and variable-order dynamics. Symmetry, 17(4), 605.

[10] Wang, C., Li, Y., Yang, G., & Deng, Q. (2025). A review of fractional-order chaotic systems of memristive neural networks. Mathematics, 13(10), 1600.

[11] Elbadri, M., Al-kuleab, N., Saadeh, R., Hafez, M., & Abdoon, M. A. (2026). Dynamics and chaos analysis of the fractional-order Lü system using a hybrid approach. Fractal and Fractional, 10(1), 51.

[12] Ding, W., Patnaik, S., Sidhardh, S., & Semperlotti, F. (2021). Applications of distributed-order fractional operators: A review. Entropy, 23(1), 110.

[13] Almutairi, D. K., AlMutairi, D. M., Taha, N. E., Dafaalla, M. E., & Abdoon, M. A. (2025). Variable-fractional-order Nosé–Hoover system: Chaotic dynamics and numerical simulations. Fractal and Fractional, 9(5), 277.

[14] Cao, Y., Sun, M., Shen, Q., & Liu, X. (2025). A variable-order nonlinear discrete grey multivariate model with new information priority accumulation and its applications. Journal of Grey System, 37(3).

[15] Patnaik, S., & Semperlotti, F. (2020). Application of variable-and distributed-order fractional operators to the dynamic analysis of nonlinear oscillators. Nonlinear Dynamics, 100(1), 561–580.

[16] Patnaik, S., Hollkamp, J. P., & Semperlotti, F. (2020). Applications of variable-order fractional operators: A review. Proceedings of the Royal Society A: Mathematical, Physical and Engineering Sciences, 476(2234).

[17] Saadeh, R., Taha, N. E., Hafez, M., Al-Mutairi, G. S., & Ashmaig, M. A. (2026). Dynamics and solution behavior of the variable-order fractional Newton–Leipnik system. Mathematics, 14(2), 312.

[18] Souid, M. S., & Benkerrouche, A. (2026). Nonlinear fractional differential equations of variable order. CRC Press.

[19] Zhang, M., & Zheng, X. (2023). Numerical approximation to a variable-order time-fractional Black–Scholes model with applications in option pricing. Computational Economics, 62(3), 1155–1175.

[20] Kothari, K., Mehta, U. V., & Prasad, R. (2019). Fractional-order system modeling and its applications. Journal of Engineering Science and Technology Review, 12(6), 1–10.

[21] Meng, R., Cao, L., & Zhang, Q. (2023). Study on the performance of variable-order fractional viscoelastic models to the order function parameters. Applied Mathematical Modelling, 121, 430–444.

[22] Sabermahani, S., Ordokhani, Y., & Hassani, H. (2021). General Lagrange scaling functions: Application in general model of variable order fractional partial differential equations. Computational and Applied Mathematics, 40(8), 269.

[23] Atangana, A. (2017). Fractional operators with constant and variable order with application to geo-hydrology. Academic Press.

[24] Ahmed, A. I., Elbadri, M., Alotaibi, A. M., Ashmaig, M. A., Dafaalla, M. E., & Kadri, I. (2025). Chaos and dynamic behavior of the 4D hyperchaotic Chen system via variable-order fractional derivatives. Mathematics, 13(20), 3240.

[25] Izadi, M., & Srivastava, H. M. (2023). Applications of modified Bessel polynomials to solve a nonlinear chaotic fractional-order system in the financial market: Domain-splitting collocation techniques. Computation, 11(7), 130.

[26] Aloui, A., Diabi, L., Kahouli, O., Ouannas, A., El Amraoui, L., & Ayari, M. (2025). Dynamic analysis of a fractional-order economic model: Chaos and control. Fractal and Fractional, 9(11), 724.

[27] Ahmed, K. I., Adam, H. D., Almutairi, N., & Saber, S. (2024). Analytical solutions for a class of variable-order fractional Liu system under time-dependent variable coefficients. Results in Physics, 56, 107311.

[28] Ma, S., Xu, Y., & Yue, W. (2012). Numerical solutions of a variable-order fractional financial system. Journal of Applied Mathematics, 2012(1), 417942.

[29] Xu, Y., & He, Z. (2013). Synchronization of variable-order fractional financial system via active control method. Central European Journal of Physics, 11(6), 824–835.

[30] Soradi-Zeid, S., Jahanshahi, H., Yousefpour, A., & Bekiros, S. (2020). King algorithm: A novel optimization approach based on variable-order fractional calculus with application in chaotic financial systems. Chaos, Solitons & Fractals, 132, 109569.

[31] Almheidat, M., Alqudah, M., Israr, M., & Ayub, A. (2025). A physics-guided deep neural network approach for simulating variable-order fractional chaotic financial models. Digital Signal Processing, 105621.

[32] Jun-hai, M., & Yu-shu, C. (2001). Study for the bifurcation topological structure and the global complicated character of a kind of nonlinear finance system (I). Applied Mathematics and Mechanics, 22(11), 1240–1251.

[33] M. S. Abd-Elouahab, N.-E. Hamri, J. Wang, Chaos control of a fractional-order

financial system, Mathematical Problems in Engineering 2010 (1) (2010) 270646.

[34] Diethelm, K., Garrappa, R., Giusti, A., & Stynes, M. (2020). Why fractional derivatives with nonsingular kernels should not be used. Fractional Calculus and Applied Analysis, 23(3), 610–634.

[35] Ghosh, I., & Fatoyinbo, H. O. (2025). Fractional order induced bifurcations in Caputo-type denatured Morris–Lecar neurons. Communications in Nonlinear Science and Numerical Simulation, 150, 108984.

[36] Almeida, R., Tavares, D., & Torres, D. F. (2019). The variable-order fractional calculus of variations. Springer.

[37] Atangana, A., & Baleanu, D. (2016). New fractional derivatives with nonlocal and non-singular kernel: Theory and application to heat transfer model. arXiv preprint arXiv:1602.03408.

[38] Atangana, A., & Owolabi, K. M. (2018). New numerical approach for fractional differential equations. Mathematical Modelling of Natural Phenomena, 13(1), 3.

[39] Toufik, M., & Atangana, A. (2017). New numerical approximation of fractional derivative with non-local and non-singular kernel: Application to chaotic models. The European Physical Journal Plus, 132(10), 444.

[40] Solís-Pérez, J. E., Gómez-Aguilar, J. F., & Atangana, A. (2018). Novel numerical method for solving variable-order fractional differential equations with power, exponential and Mittag-Leffler laws. Chaos, Solitons & Fractals, 114, 175–185.

[41] Ahmed, A. I., Elbadri, M., Alotaibi, A. M., Ashmaig, M. A., Dafaalla, M. E., & Kadri, I. (2025). Chaos and dynamic behavior of the 4D hyperchaotic Chen system via variable-order fractional derivatives. Mathematics, 13(20), 3240.

[42] El Guma, F., Abdoon, M. A., Abdalla, S. J. M., Alharbi, S. A., Alsemiry, R. D., Allogmany, R., & Al-Kuleab, N. (2025). Fractional-order modeling of influenza dynamics: Impact of memory effect and severity-based variations. International Journal of Biomathematics, 2550127.

[43] Zhuang, P., Liu, F., Anh, V., & Turner, I. (2009). Numerical methods for the variable-order fractional advection-diffusion equation with a nonlinear source term. SIAM Journal on Numerical Analysis, 47(3), 1760–1781.

[44] Kadri, I. (2025). A novel analytical solutions for systems of fractional differential equations using the conformable fractional Laplace transform method. Karshi Multidisciplinary International Scientific Journal, 2(2), 65–71.